Supplement of Atmos. Chem. Phys., 24, 2985–3007, 2024
https://doi.org/10.5194/acp-24-2985-2024-supplement

Atmospheric Chemistry and Physics
Open Access
EGU

Supplement of

Improved estimates of smoke exposure during Australia fire seasons: importance of quantifying plume injection heights

Xu Feng et al.

Correspondence to: Xu Feng (xfeng@g.harvard.edu)

S1: Definition of the plume injection height parameters

The Global Fire Assimilation System (GFAS, Rémy et al., 2017) relies on a 1-D plume rise model (Freitas et al., 2007, 2010) to calculate the top of the plume, the bottom of the plume, and the mean height of maximum injection (MHMI). This plume rise model is governed by equations based on the vertical motion, mass conservation, and the first thermodynamic law (Freitas et al., 2007). A schematic of this plume rise model is shown in Figure 1 of Rémy et al. (2017). The plume entrainment and detrainment profiles are estimated by functions of fire radiative power, fire area, ambient temperature, and wind profiles. The detrainment is used to define the MHMI, which is the average of plume heights where detrainment exceeds half of the maximum value. The heights of the top and bottom of the detrainment profile are defined as the top and bottom heights of the plume.

GFAS also relies on a semi-empirical parameterization IS4FIRES (Sofiev et al., 2012, 2013) to calculate the injection height, which is defined as the top of the plume. According to this algorithm (Eq. S1), the top of the plume (H_p) is a function of the PBL height (H_{abl}), fire radiative power (FRP), and Brunt-Vaisala frequency in the free troposphere (N_{FT}). The other coefficients are constant values.

$$H_p = \alpha H_{abl} + \beta \left(\frac{FRP}{P_{f0}}\right)^{\gamma} exp\left(\frac{-\delta N_{FT}^2}{N_0^2}\right) \quad (S1)$$

S2: Digitization of plume heights using MINX

The key input data for MINX is MISR Level 1 terrain-referenced imagery (L1B2 Terrain Radiance, Diner et al., 1998; Jovanovic et al., 1998). Given the perimeter and direction of each plume in the MISR imagery, MINX digitizes the plume height, wind speed, and terrain height at each pixel within the identified plume perimeter. The algorithm computes both zero-wind height and wind-corrected height at each pixel. For zero-wind heights, the apparent plume motions observed by different viewing angles are assumed to be entirely due to parallax; for wind-corrected heights, the heights are adjusted to consider plume advection by local winds (Nelson et al., 2013). The mean number of valid pixels of retrieved zero-wind heights per plume over Australia is 200, greater than that of wind-corrected heights (120 valid pixels). The reason for this difference may be traced to missing values in the wind fields used for correction. In our study, we use the zero-wind heights to calculate the vertical profile for each plume.

S3: Algorithm of the STILT model

The STILT algorithm releases an ensemble of air parcels at a receptor and tracks the trajectory of each air parcel backwards in time for a specified number of days. As shown in Eq. (S1), the concentration change

(ΔC, in units of ppm) at the receptor (x_r, y_r) at time t_r due to the surface emission flux (F, in units of μmol m^{-2} s^{-1}) from a source point (x_i, y_j) is determined by the total amount of time ($\Delta t_{p,i,j,k}$) that each air parcel stays in the volume element (i, j, k) during the time step t_m, the total number of air parcels (N_{tot}), and the diluting height (h). STILT assumes that surface emission fluxes are instantaneously diluted into an atmospheric column of h due to turbulent mixing. The average density of all air parcels below h is $\overline{\rho}$, and m_{air} is the air molecular weight. The diluting height h is generally set to be within the PBL, and STILT assumes that emission fluxes distributed above h do not affect surface concentrations downwind (Lin et al., 2003; Gerbig et al., 2003). The definition of sensitivity footprints is given in Eq. (S2) with units of ppm μmol^{-1} m^2 s.

$$\Delta C\left(x_r, y_r, t_r \middle| x_i, y_j, t_m\right) = \begin{cases} \dfrac{m_{air}}{h\overline{\rho}(x_i, y_j, t_m)} \dfrac{1}{N_{tot}} \displaystyle\sum_{p=1}^{N_{tot}} \Delta t_{p,i,j,k} \cdot F(x_i, y_i, t_m), & z \le h \\ 0, & z > h \end{cases} \quad (S1)$$

$$f\left(x_r, y_r, t_r \middle| x_i, y_j, t_m\right) = \frac{m_{air}}{h\overline{\rho}(x_i, y_j, t_m)} \frac{1}{N_{tot}} \sum_{p=1}^{N_{tot}} \Delta t_{p,i,j,k} \quad (S2)$$

Table S1. Statistics for seasonal-mean $PM_{2.5}$ concentrations simulated by three simulations, compared to the ground-based observations at 12 receptors. CTL is the control simulation, INJ-CLIM represents the climatological method of calculating plume height, and INJ-RF represents the method using random forest. The observation site name in each city or town is given in parentheses.

Cities (site)	**Observation periods (Locations)**	***R*[a]**			**NMB**			**RMSE (μg m^{-3})**		
		CTL	***INJ-CLIM***	***INJ-RF***	***CTL***	***INJ-CLIM***	***INJ-RF***	***CTL***	***INJ-CLIM***	***INJ-RF***
Darwin [b] (Palmerston)	2011-2020 (130.94°E, 12.50°S)	0.78	0.54	0.77	16.7%	-18.0%	-2.5%	2.8	2.7	1.7
Gladstone [c] (South Gladstone)	2009-2020 (151.27°E, 23.86°S)	0.86	0.88	0.88	-5.8%	-11.4%	-11.7%	1.0	1.1	1.1
Brisbane [c] (Springwood)	2009-2020 (153.13°E, 27.61°S)	0.60	0.54	0.61	6.3%	-5.6%	-10.0%	1.4	1.3	1.3
Newcastle [d] (Wallsend)	2009-2020 (151.66°E, 32.89°S)	0.91	0.92	0.91	4.5%	-5.1%	-11.2%	3.5	1.8	1.5
Sydney [d] (Liverpool)	2009-2020 (150.90°E, 33.93°S)	0.96	0.95	0.95	3.3%	-2.6%	-7.2%	1.9	1.1	1.1
Wollongong [d] (Wollongong)	2009-2020 (150.88°E, 34.41°S)	0.86	0.85	0.80	-4.4%	-8.6%	-11.2%	1.2	1.3	1.6
Melbourne [e] (Footscray)	2009-2020 (144.87°E, 37.80°S)	0.48	0.47	0.40	2.3%	1.7%	-1.8%	1.3	1.3	1.3
Melbourne [e] (Alphington)	2009-2020 (145.03°E, 37.77°S)	0.61	0.61	0.67	14.7%	14.1%	8.5%	1.7	1.6	1.3
Albury [d] (Albury)	2017-2020 (146.93°E, 36.05°S)	0.98	0.98	0.97	-25.5%	-26.6%	-32.2%	5.3	5.5	6.5
Canberra [f] (Florey)	2014-2020 (149.04°E, 35.22°S)	0.99	0.99	0.99	16.1%	-7.4%	-13.6%	7.0	1.4	1.8
Sydney [d] (Prospect)	2014-2020 (150.91°E, 33.79°S)	0.99	0.99	0.99	1.7%	-4.7%	-9.2%	1.6	0.69	0.98
Newcastle [d] (Newcastle)	2014-2020 (151.75°E, 32.93°S)	0.91	0.89	0.91	19.0%	4.8%	-3.3%	4.2	2.0	1.4

[a] Temporal correlation coefficient between the observed and simulated annual mean total $PM_{2.5}$ concentrations during the fire seasons (April to December for Darwin and Gladstone; August to December for other cities).
[b] Observation data source: Northern Territory Environment Protection Authority (http://ntepa.webhop.net/NTEPA/Default.ltr.aspx)
[c] Queensland Government Open Data Portal (https://apps.des.qld.gov.au/air-quality/download/)
[d] New South Wales Department of Planning and Environment (https://www.dpie.nsw.gov.au/air-quality/air-quality-data-services/data-download-facility)
[e] Victoria Environment Protection Authority (https://www.epa.vic.gov.au/for-community/airwatch)

60 [f] Australian Capital Territory Government Open Data Portal (https://www.data.act.gov.au/Environment/Air-Quality-Monitoring-Data/94a5-zqnn

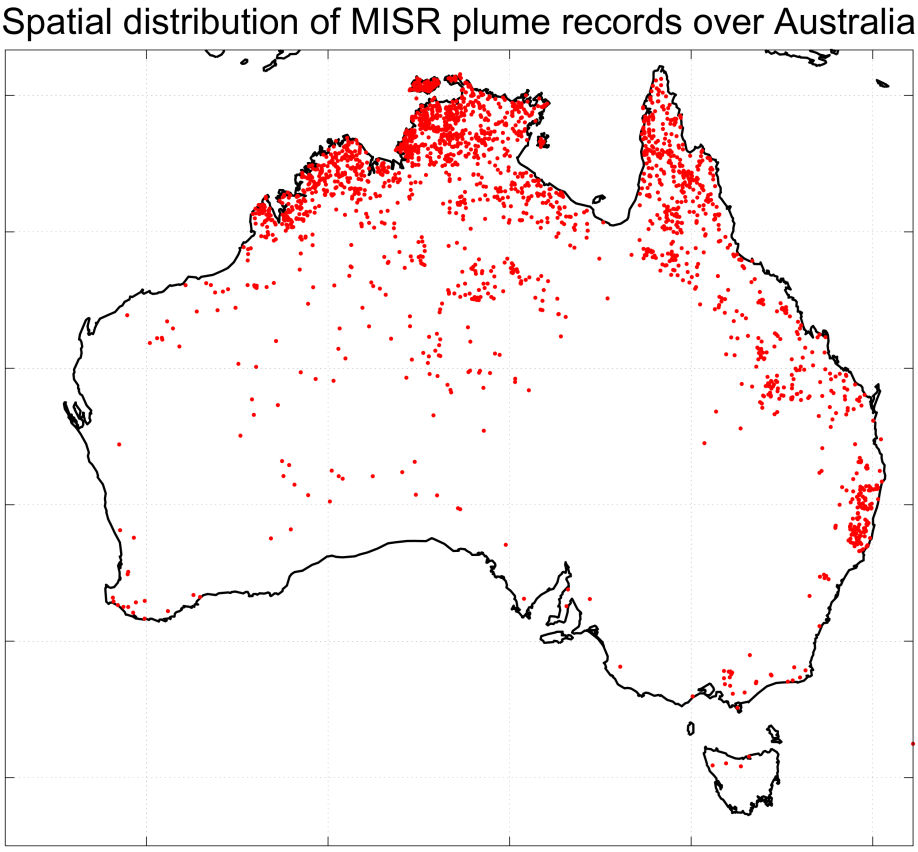

Figure S1. Spatial distribution of all MISR plume records over Australia used in this study.

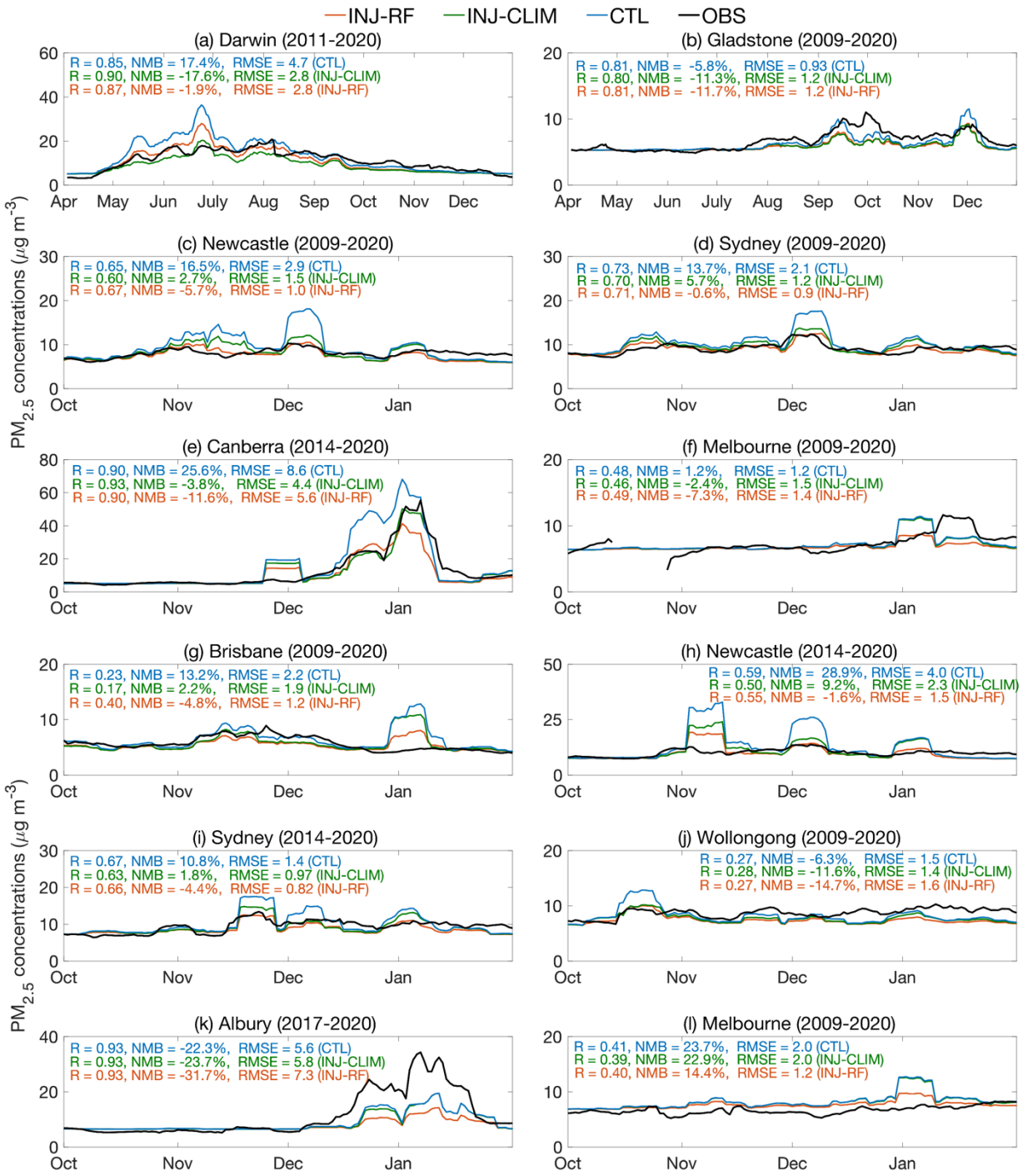

Figure S2. Time series of 10-day moving average of observed and simulated total $PM_{2.5}$ concentrations from the CTL (blue), INJ-CLIM (green), and INJ-RF (red) experiments during the fire seasons at representative receptors in 12 receptors: (a) Darwin (Palmerston), (b) Gladstone (South Gladstone), (c) Newcastle (Wallsend), (d) Sydney (Liverpool), (e) Canberra (Florey), (f) Melbourne (Footscray), (g) Brisbane (Springwood), (h) Newcastle (Newcastle), (i) Sydney (Prospect), (j) Wollongong (Wollongong), (k) Albury (Albury), and (l) Melbourne (Alphington). Given in parentheses are the names of the observation sites. The 10-day moving averages are calculated over each receptor's observing period, as indicated above

the panels. Shown inset are the temporal correlation coefficients *R*, NMBs, and RMSEs of daily total $PM_{2.5}$ concentrations compared to the surface measurements.

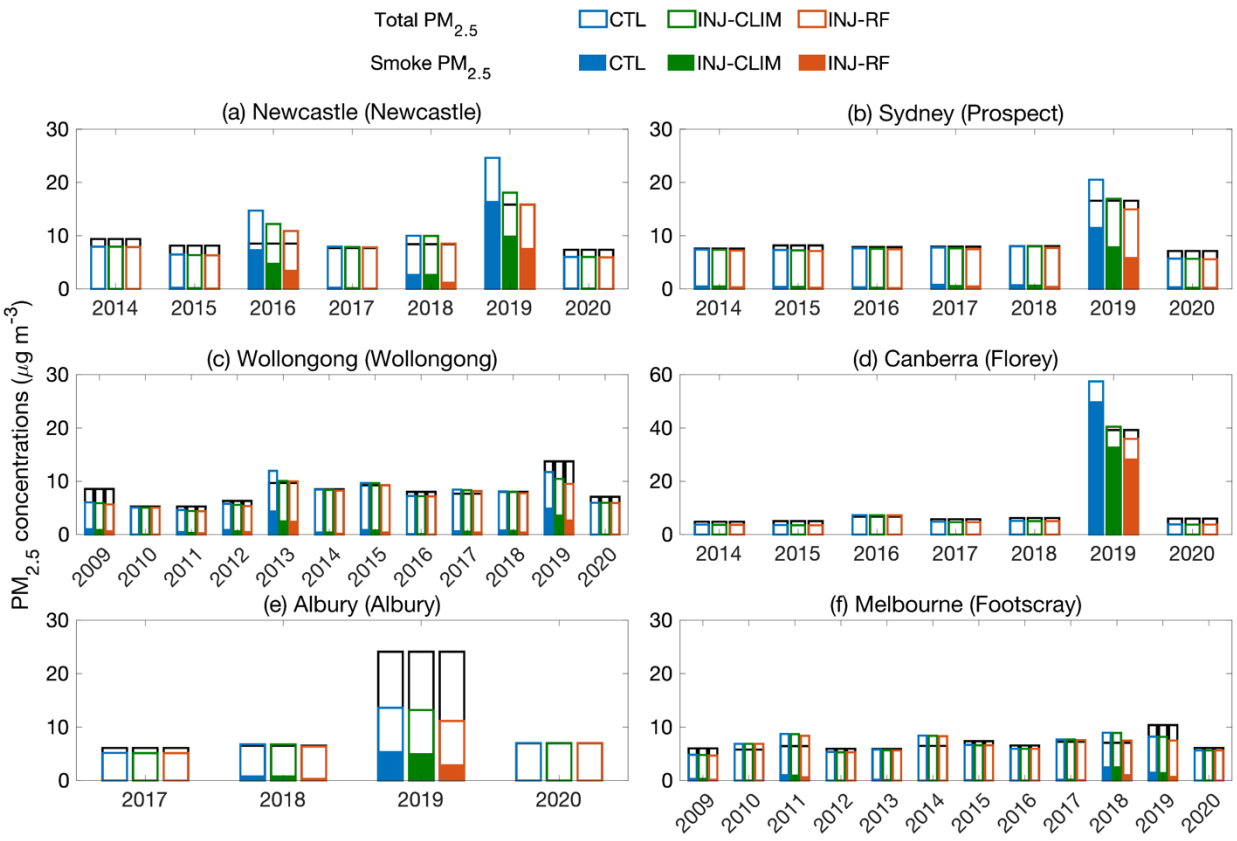

Figure S3. Mean simulated concentrations of smoke $PM_{2.5}$ and background $PM_{2.5}$ from the three sensitivity experiments (blue: CTL, green: INJ-CLIM, red: INJ-RF), as well as observed total $PM_{2.5}$ concentrations (black: OBS) in (a) Newcastle (Newcastle), (b) Sydney (Prospect), (c) Wollongong (Wollongong), (d) Canberra (Florey), (e) Albury (Albury), and (f) Melbourne (Footscray). (The names of the observation sites are given in parentheses.) The different receptors have different observation periods. The modeled total $PM_{2.5}$ concentrations are designated by the height of the colored bars, consisting of smoke $PM_{2.5}$ (color-filled bars) and the background $PM_{2.5}$ (empty bars) in units of μg m^{-3}.

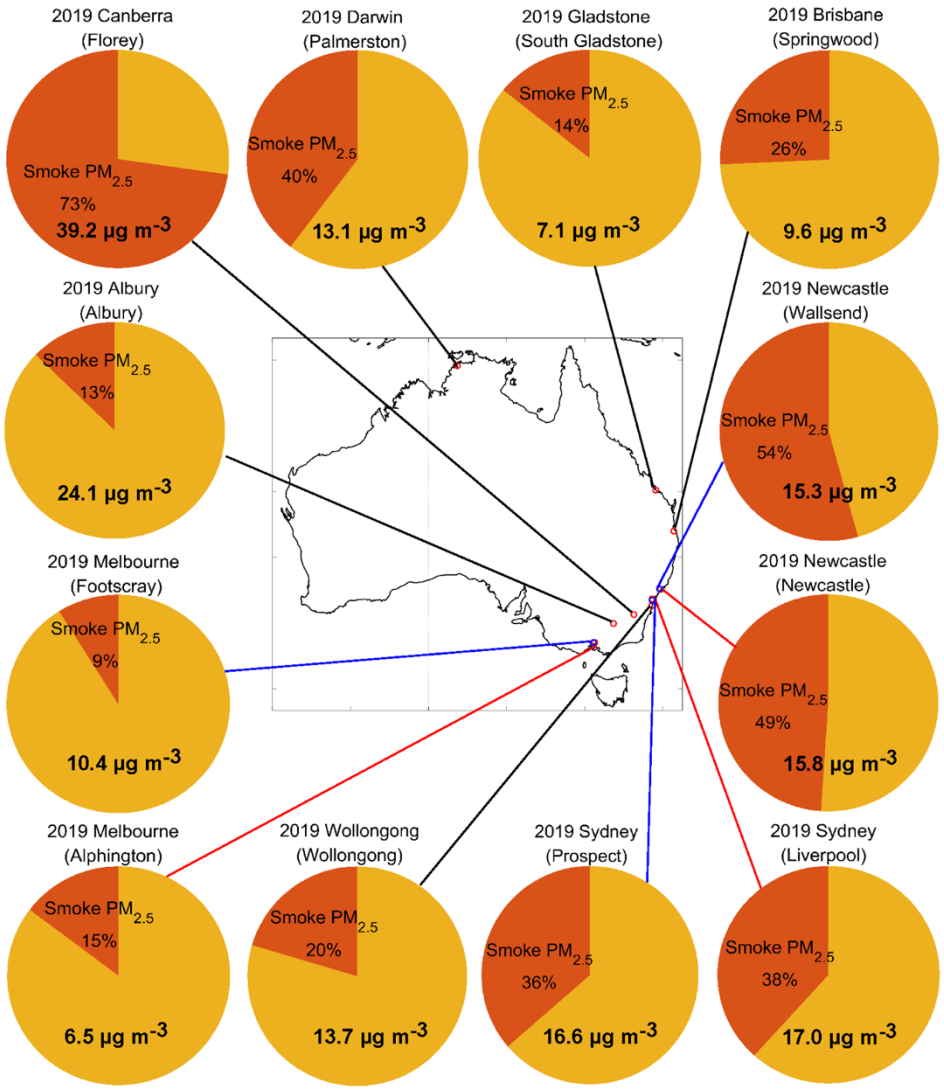

Figure S4. Contributions of simulated smoke $PM_{2.5}$ concentrations from the INJ-RF experiment to the observed total $PM_{2.5}$ concentrations (numbers on the pie charts) at 12 receptors averaged over the fire seasons of 2019. Names of the observation sites are given in parentheses. Red sectors represent smoke contributions, while dark yellow sectors signify the differences between observed total $PM_{2.5}$ and simulated smoke $PM_{2.5}$ concentrations – i.e., the non-fire $PM_{2.5}$. Small circles on map represent the locations of these receptors. Different colors (red, blue, and black) are used to distinguish adjacent receptors.

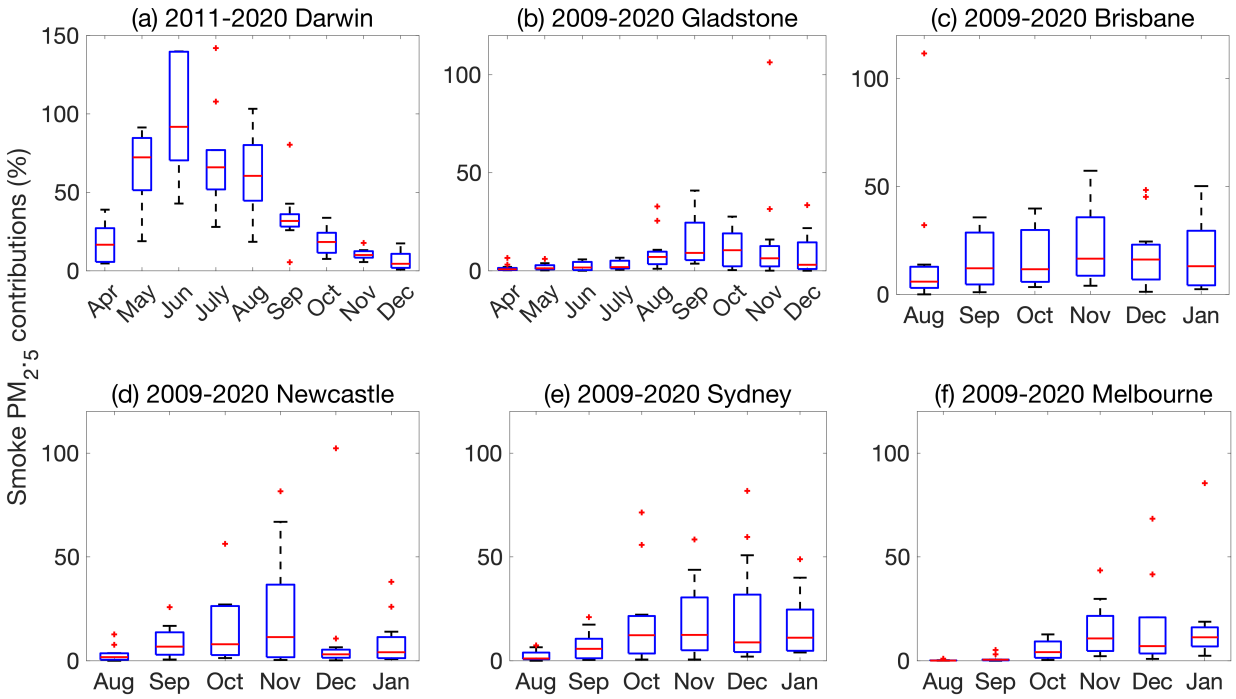

Figure S5. Boxplot of monthly contributions of simulated smoke $PM_{2.5}$ concentrations from the INJ-RF experiment to the observed total $PM_{2.5}$ concentrations during respective observation periods in (a) Darwin (Palmerston), (b) Gladstone (South Gladstone), (c) Brisbane (Springwood), (d) Newcastle (Wallsend), (e) Sydney (Liverpool), and (f) Melbourne (Alphington). The bottom, top, and red line in the middle of each box are the 25th and 75th percentiles, as well as the median of all data. The distance between the 75th and 25th percentiles is the interquartile range. The lower and upper whisker limits represent the most extreme data values within 1.5 times the interquartile range. The data greater than 1.5 times outside the interquartile range are considered outliers and are shown as the red crosses. In some years, the monthly smoke $PM_{2.5}$ contributions over 100% are due to the overestimates of simulated smoke $PM_{2.5}$.